

# Characterization of the effect of joint clearance on the energy loss of flexible multibody systems with variable kinematic structure

Saeed Ebrahimi<sup>\*1</sup>, Esmail Salahshoor<sup>1a</sup> and Shapour Moradi<sup>2b</sup>

<sup>1</sup>Department of Mechanical Engineering, Yazd University, Yazd, Iran

<sup>2</sup>Department of Mechanical Engineering, Shahid Chamran University of Ahvaz, Ahwaz, Iran

(Received June 3, 2016, Revised July 22, 2017, Accepted July 26, 2017)

**Abstract.** Clearances are essential for the assemblage of mechanisms to allow the relative motion between the joined bodies. This clearance exists due to machining tolerances, wear, material deformations, and imperfections, and it can worsen the mechanism performance when the precision and smoothly-working are intended. Energy is a subject which is less paid attention in the area of clearance. The effect of the clearance on the energy of a flexible slider-crank mechanism is investigated in this paper. A clearance exists in the joint between the slider and the coupler. The contact force model is based on the Lankarani and Nikravesh model and the friction force is calculated using the modified Coulomb's friction law. The hysteresis damping which has been included in the contact force model dissipates energy in clearance joints. The other source for the energy loss is the friction between the journal and the bearing. Initial configuration and crank angular velocity are changed to see their effects on the energy of the system. Energy diagrams are plotted for different coefficients of friction to see its influence. Finally, considering the coupler as a flexible body, the effect of flexibility on the energy of the system is investigated.

**Keywords:** clearance; energy loss; flexibility; floating frame of reference

## 1. Introduction

In multibody systems, kinematic joints are generally assumed to be ideal i.e., without clearance. In real mechanical joints, there is a distance between journal and bearing. This clearance exists due to machining tolerances, wear, material deformations, and imperfections, and it can worsen the mechanism performance when the precision and smoothly-working are intended. This is because of the impact forces applied between the journal and the bearing.

Three main types of clearance model could be found in the literature, namely, the massless link approach, the spring-damper approach, and the momentum exchange approach. In the momentum exchange approach, which is used in this research, the clearance is modeled as two colliding bodies. There will be no kinematic constraints between the journal and the bearing and the impact-contact force between them controls the dynamic behavior of the system. These impacts in the clearance joint lead to high contact force and consequently high acceleration. This model is more realistic than two other approaches, because it considers the contact forces as a function of surface elasticity in addition to taking into account the energy dissipation during impact (Flores and Ambrosio 2004).

The contact problem is a challenging subject in mechanical systems. This phenomenon is greatly paid

attention in the literature (see for example Garrido *et al.* 1994, Liu and Yang 1998, Li *et al.* 2015, Oner *et al.* 2015 and Gandhi *et al.* 2015). Contact happens repeatedly in multibody systems with clearance. Clearance in mechanical joints has attracted many researchers in recent decades. Dubowsky and Freudenstein (1971) used impact pair model for joint clearance. In their model, contact surface was considered as a spring-damper element which was apart from the other surface as far as the clearance size. In addition, Rhee and Akay (1996) investigated the response of a four-bar mechanism with a clearance joint and showed that a nonlinear dependence on both the clearance size and the coefficient of the friction between the journal and the bearing exists. In addition, the pin trajectories and the Poincare maps indicated that the motion of the pin can be simple periodic, periodic motions with periods that are multiples of the crank revolution and in some cases, it can be chaotic. It was also presented that at moderately high coefficient of friction, the pin motion is simple periodic with a period the same as that of crank rotation. Ravn (1998) analyzed a slider-crank mechanism with a clearance in joint between the coupler and the slider. He used the continuous contact force model in which the contact force was a function of the amount of penetration between journal and bearing. This force controls the dynamic behavior of the journal and the bearing. Schwab *et al.* (2002) made a comparison between several continuous contact force models and an impact model. It was achieved that the compliance of the links or lubrication of the joint smooths the peak values of the contact forces. Flores *et al.* (2004) investigated the clearance in a multibody system considering lubrication. The compressive force applied by the lubricant, when there is no contact between journal and

\*Corresponding author, Associate Professor  
E-mail: ebrahimi@yazd.ac.ir

<sup>a</sup>Ph.D. Student

<sup>b</sup>Professor

bearing, was taken into account in the equations of motion. Khemili and Romdhane (2008) studied the dynamic behavior of a planar flexible slider-crank mechanism with clearance. Simulation and experimental tests were carried out and the model was built under the software ADAMS for the simulation tests. It was shown that in the presence of clearance, the coupler flexibility has a role of suspension for the mechanism. Mukras *et al.* (2010) presented a procedure to analyze planar multibody systems in which wear occurs at one or more revolute joints. The wear was computed based on Archard's wear model and validated with an experimental slider-crank mechanism. The wear in clearance joints is also investigated in other papers (Feng *et al.* 2013, Zhao *et al.* 2013, Pei *et al.* 2013). Zhang *et al.* (2014) analyzed a 3-RRR parallel mechanism with six clearance joints. They showed that the joint clearances have considerable effects on the displacement and velocity of the moving platform, and have great influence on the acceleration and driving moments. Zhang *et al.* (2015) presented a multiobjective problem in which the effect of the clearance on the slider acceleration, contact force and power consumption was investigated. For more papers on the optimization of the mechanical systems with clearance, the reader is referred to (see for example Erkaya and Uzmay 2009, Sardashti *et al.* 2013, Varedi 2015). The interested reader could refer to many other researches dealing with clearance joint such as (Lankarani and Nikravesh 1994, Qiang Tian *et al.* 2009, 2010, 2011, 2013, 2015).

In addition to the researches related to the modeling of the clearance, vibrational analysis of the mechanical systems with clearance is also considered in the literature. Vaidya and Padole (2010) considered a four-bar linkage with clearance. They modeled the bearing stiffness as a linear and torsional spring and added this stiffness to the assembled stiffness matrix to find out the effect of joint flexibility on natural frequencies. In addition, Zhao *et al.* (2016) used a hybrid method for identifying the bearing joint stiffness of high speed spindles which can effectively have influence on its dynamic characteristics. The bearing stiffness was modeled based on the Hertz contact theory. Erkaya (2012) investigated the effect of the clearance on the vibration of the bearing of a slider-crank mechanism. He designed a neural network for the different clearance sizes and velocities. He collected the data from three accelerometers to find out the vibration of the system. Time, clearance size, velocity and the material of the mechanism were the network inputs and three accelerometers data were its outputs. Yang *et al.* (2012) investigated the vibrational modes of a cantilever beam with a block mounted on it with a clearance. Ebrahimi *et al.* (2017a) tried to find the instantaneous natural frequencies of a flexible fourbar mechanism with a single clearance joint. Salahshoor *et al.* (2016), Ebrahimi *et al.* (2017b) tried to obtain an analytical solution for a mechanical system with clearance joint using multiple scales method. Due to the high nonlinearity of the clearance joint behavior, some effort has been devoted to the investigation of the chaos and bifurcation in multibody systems with clearance (see for example Chunmei *et al.* 2002, Rahmanian and Ghazavi 2015).

Although there is a vast amount of researches on

modeling of the clearance and its effect on the dynamic behavior of the multibody systems, very little attention has been paid to the energy of the systems with clearance joints. The major contribution of this work is devoted to the effect of clearance on the energy of the system. At first, a rigid slider-crank mechanism which has a clearance joint between the slider and the coupler is used as a demonstrative sample. The clearance is modeled using the momentum exchange approach. The continuous contact force model is used to evaluate the contact force and the friction force is achieved by the modified Coulomb's friction law. Energy of the system for different initial crank angular velocity and various coefficients of friction is presented. Finally, the coupler is considered as a flexible body and its effect on the energy of the system is investigated when there is clearance in the system. The floating frame of reference formulation is used to model the flexible coupler and Rayleigh damping is assumed for the damping of the flexible body.

## 2. Multibody system dynamics

### 2.1 Equations of motion for rigid multibody systems

A multibody system is defined as a set of interconnected rigid bodies that can have large displacements and rotations. In order to determine the position and orientation of a rigid body, a coordinate system is attached to that body. The origin of this body-fixed coordinate system is specified with respect to the global coordinate system as

$$\mathbf{q}_i = [R_{x_i} \ R_{y_i} \ \theta_i]^T \quad (1)$$

where  $\theta_i$  is the relative angle between the body reference frame and the global coordinate system,  $R_{x_i}$  and  $R_{y_i}$  determine the position of the body reference frame origin with respect to the global coordinate system. There are some constraints between two adjacent bodies which are connected by means of joints. These constraints are expressed as

$$\mathbf{C}(\mathbf{q}, t) = \mathbf{0} \quad (2)$$

where  $\mathbf{q}$  is a set of generalized coordinates which specify the position and orientation of all the bodies of the multibody system. If the number of the constraints equals to the number of the generalized coordinates, the system is said to be kinematically driven (Shabana 2001). Differentiating Eq. (2) yields two equations through which velocities and accelerations are achieved

$$\mathbf{C}_q \dot{\mathbf{q}} = -\mathbf{C}_t \quad (3)$$

$$\mathbf{C}_q \ddot{\mathbf{q}} = -(\mathbf{C}_q \dot{\mathbf{q}})_q \dot{\mathbf{q}} - 2\mathbf{C}_{qt} \dot{\mathbf{q}} - \mathbf{C}_{tt} = \mathbf{Q}_d \quad (4)$$

where  $\mathbf{C}_q$  is the Jacobian matrix and is a square matrix for a kinematically driven system. However, if the number of constraints is less than the number of degrees of freedom, the force analysis is required and the equations of motion are expressed as

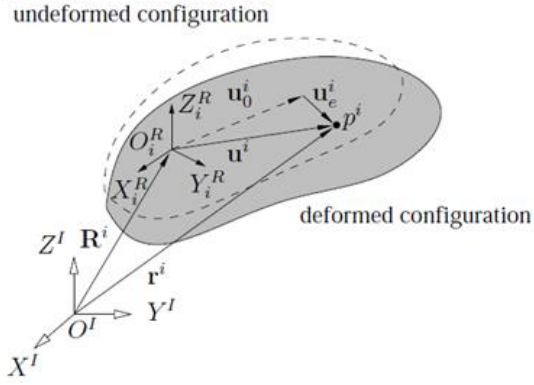


Fig. 1 Flexible body kinematics (Ebrahimi 2007)

$$\begin{bmatrix} \mathbf{M} & \mathbf{C}_q^T \\ \mathbf{C}_q & \mathbf{0} \end{bmatrix} \begin{bmatrix} \ddot{\mathbf{q}} \\ \lambda \end{bmatrix} = \begin{bmatrix} \mathbf{Q}_e \\ \mathbf{Q}_d \end{bmatrix} \quad (5)$$

where  $\mathbf{M}$  is the mass matrix,  $\ddot{\mathbf{q}}$  is the acceleration vector,  $\lambda$  is the vector of Lagrange multipliers and  $\mathbf{Q}_e$  is the generalized force vector which is calculated when the external force applies to the system.

## 2.2 Flexibility modeling

Traditionally, dynamic analysis of multibody systems was based on the rigid body assumption. This assumption is correct for a multibody system operating at low speeds and when the links behave as rigid bodies. But when the systems operate at higher speeds, the links deform considerably and the rigid body assumption is no longer valid. Dynamic analysis of elastic bodies is much different from that of rigid ones (Jablonkow *et al.* 1993).

### 2.2.1 Floating frame of reference

The floating frame of reference approach is the most widely used method in flexible multibody dynamics. However, its use has been confined to applications in which the deformation of the body with respect to its coordinate system is assumed to be small. In this approach, configuration of each flexible body in the multibody system is specified by using two sets of coordinates: reference and elastic coordinates. Reference coordinates define the location and orientation of a body reference attached to the elastic body. Elastic coordinates determine the body deformation with respect to the body reference (Shabana 2005). To explain the floating frame of reference formulation in more details, consider Fig. 1 which shows inertial and body reference frames necessary for determining the position of all points of the body  $i$ .

Therefore, the position of an arbitrary point  $p^i$  is expressed as

$$\begin{aligned} \mathbf{r}_p^i &= \mathbf{R}^i + \mathbf{u}^i = \mathbf{R}^i + \mathbf{A}^i \bar{\mathbf{u}}^i = \\ \mathbf{R}^i + \mathbf{A}^i (\bar{\mathbf{u}}_o^i + \bar{\mathbf{u}}_e^i) &= \mathbf{R}^i + \mathbf{A}^i (\bar{\mathbf{u}}_o^i + \mathbf{S}^i \mathbf{q}_e^i) \end{aligned} \quad (6)$$

where  $\mathbf{A}^i$  is the transformation matrix,  $\bar{\mathbf{u}}^i$  is the local position vector of point  $p$ ,  $\bar{\mathbf{u}}_o^i$  is the position of point  $p$  in

the undeformed state,  $\mathbf{S}^i$  is a space-dependent shape matrix, and  $\mathbf{q}_e$  is the vector of time-dependent elastic generalized coordinates of the deformable body  $i$ . The coordinates of body  $i$  can be defined as

$$\mathbf{q}^i = [\mathbf{R}^i \quad \boldsymbol{\theta}^i \quad \mathbf{q}_e^i]^T \quad (7)$$

where  $\mathbf{R}^i$  and  $\boldsymbol{\theta}^i$  are the reference coordinates and  $\mathbf{q}_e$  is the vector of elastic yields coordinates. Differentiating Eq. (6) with respect to time yields

$$\begin{aligned} \dot{\mathbf{r}}_p^i &= \mathbf{L}^i \dot{\mathbf{q}}^i \\ \mathbf{L}^i &= [\mathbf{I} \quad \mathbf{B}^i \quad \mathbf{A}^i \mathbf{S}^i] \quad \dot{\mathbf{q}}^i = [\dot{\mathbf{R}}^i \quad \dot{\boldsymbol{\theta}}^i \quad \dot{\mathbf{q}}_e^i]^T \\ \mathbf{B}^i &= \left[ \frac{\partial}{\partial \theta_1^i} (\mathbf{A}^i \bar{\mathbf{u}}^i) \quad \dots \quad \frac{\partial}{\partial \theta_{n_r}^i} (\mathbf{A}^i \bar{\mathbf{u}}^i) \right] \end{aligned} \quad (8)$$

where  $\mathbf{I}$  is a unity matrix and  $n_r$  is the number of total rotational coordinates of the reference of body  $i$ . The vector  $\dot{\mathbf{R}}^i$  is the absolute velocity vector of the origin of the body reference,  $\mathbf{A}^i \mathbf{S}^i \dot{\mathbf{q}}_e^i$  is the velocity of point  $p$  due to the deformation of the body, defined with respect to an observer placed on the body and  $\mathbf{B}^i \dot{\boldsymbol{\theta}}^i$  is the result of differentiation of the transformation matrix with respect to time. Differentiating Eq. (8) with respect to time yields

$$\ddot{\mathbf{r}}_p^i = \dot{\mathbf{L}}^i \dot{\mathbf{q}}^i + \mathbf{L}^i \ddot{\mathbf{q}}^i \quad (9)$$

where  $\dot{\mathbf{L}}^i \dot{\mathbf{q}}^i$  is a quadratic velocity vector that contains the Coriolis component. Considering the kinetic energy of a deformable body, one can obtain the mass matrix as (Shabana 2005)

$$\begin{aligned} \mathbf{M} &= \int_{V^i} \rho^i \begin{bmatrix} \mathbf{I} \\ (\mathbf{B}^i)^T \\ (\mathbf{A}^i \mathbf{S}^i)^T \end{bmatrix} [\mathbf{I} \quad \mathbf{B}^i \quad \mathbf{A}^i \mathbf{S}^i] dV^i = \\ &= \int_{V^i} \rho^i \begin{bmatrix} \mathbf{I} & \mathbf{B}^i & \mathbf{A}^i \mathbf{S}^i \\ (\mathbf{B}^i)^T \mathbf{B}^i & (\mathbf{B}^i)^T \mathbf{A}^i \mathbf{S}^i & \\ \text{symmetric} & (\mathbf{S}^i)^T \mathbf{S}^i & \end{bmatrix} dV^i \end{aligned} \quad (10)$$

The equations of motion and the constraints can be expressed as a matrix equation similar to Eq. (5)

$$\begin{bmatrix} \mathbf{M} & \mathbf{C}_q^T \\ \mathbf{C}_q & \mathbf{0} \end{bmatrix} \begin{bmatrix} \ddot{\mathbf{q}} \\ \lambda \end{bmatrix} = \begin{bmatrix} \mathbf{Q}_e + \mathbf{Q}_v - \mathbf{K}\mathbf{q} - \mathbf{D}\dot{\mathbf{q}} \\ \mathbf{Q}_d \end{bmatrix} \quad (11)$$

where  $\mathbf{D}$  is the damping matrix,  $\mathbf{Q}_v$  is the quadratic velocity vector and  $\mathbf{K}$  is the stiffness matrix of the body  $i$ . The quadratic velocity vector and the stiffness matrix are obtained as (Shabana 2005)

$$\begin{aligned} \mathbf{Q}_v^i &= -\dot{\mathbf{M}}^i \dot{\mathbf{q}}^i + \frac{1}{2} \left[ \frac{\partial}{\partial \dot{\mathbf{q}}^i} (\dot{\mathbf{q}}^{iT} \mathbf{M}^i \dot{\mathbf{q}}^i) \right]^T \\ \mathbf{K} &= \begin{bmatrix} 0 & 0 & 0 \\ 0 & 0 & 0 \\ 0 & 0 & \mathbf{K}_{ee}^i \end{bmatrix}, \quad \mathbf{K}_{ee}^i = \int_{V^i} (\mathbf{D}^i \mathbf{S}^i)^T \mathbf{E}^i \mathbf{D}^i \mathbf{S}^i dV^i \end{aligned} \quad (12)$$

where  $\mathbf{D}^i$  is a differential operator that relates the strain vector to the deformation vector and  $\mathbf{E}^i$  is the symmetric matrix of elastic coefficients. The damping coefficient matrix is sometimes approximated with a so-called proportional or Rayleigh damping as a linear combination of the mass matrix and the stiffness matrix (see Ebrahimi 2007 and Ebrahimi *et al.* 2008)

$$\mathbf{D} = \begin{bmatrix} 0 & 0 & 0 \\ 0 & 0 & 0 \\ 0 & 0 & [d_{ee}] \end{bmatrix}, d_{ee} = \alpha m_{ee} + \beta k_{ee} \quad (13)$$

where  $\alpha$  and  $\beta$  are two constant parameters, which can be determined from two given damping ratios  $\zeta_1$  and  $\zeta_2$  that correspond to two different frequencies  $\omega_1$  and  $\omega_2$

$$\alpha = \frac{2\omega_1\omega_2}{\omega_2^2 - \omega_1^2} (\zeta_1\omega_2 - \zeta_2\omega_1), \quad (14)$$

$$\beta = \frac{2}{\omega_2^2 - \omega_1^2} (\zeta_2\omega_2 - \zeta_1\omega_1)$$

$m_{ee}$  is the mass matrix element associated with the elastic coordinates. For determining  $\omega_1$  and  $\omega_2$ , the procedure presented in (Bathe 1996) is used in this paper.

### 3. Clearance modeling

Three main types of clearance model could be found in the literature, namely, the massless link approach, the spring-damper approach, and the momentum exchange approach. In this paper, the third model, the momentum exchange approach, which is more realistic, is used. In this approach, the constraint equation between two bodies is cancelled and the contact force controls the dynamic behavior of the colliding journal and bearing. Three conditions are expected during motion, free flight motion, impact mode and continuous contact mode. In the free flight motion, the journal moves freely inside the bearing boundary and there is no contact. At the end of the free flight motion, impact mode could happen in which the contact forces are applied and removed in the system and there will be a discontinuity in the kinematic and dynamic characteristics. A sudden change will occur in the momentum of the colliding bodies. In the continuous contact mode, there will be a permanent contact between the journal and the bearing and a sliding motion exists. The contact force proposed by Lankarani and Nikravesh is expressed as

$$F_N = K \delta^n \left( 1 + \frac{3(1-e_r^2)}{4} \frac{\dot{\delta}}{\delta^{(-)}} \right) \quad (15)$$

$$K = \frac{4}{3(h_i + h_j)} \left( \frac{R_i R_j}{R_i + R_j} \right)^{\frac{1}{2}} \quad h_k = \frac{1 - \nu_k^2}{E_k} \quad k = i, j$$

where  $F_N$  is the normal contact force,  $K$  is a constant depending on the material properties and geometry of the colliding bodies,  $\delta$  is the penetration between the journal and the bearing,  $e_r$  is the coefficient of the restitution,  $\dot{\delta}$  is

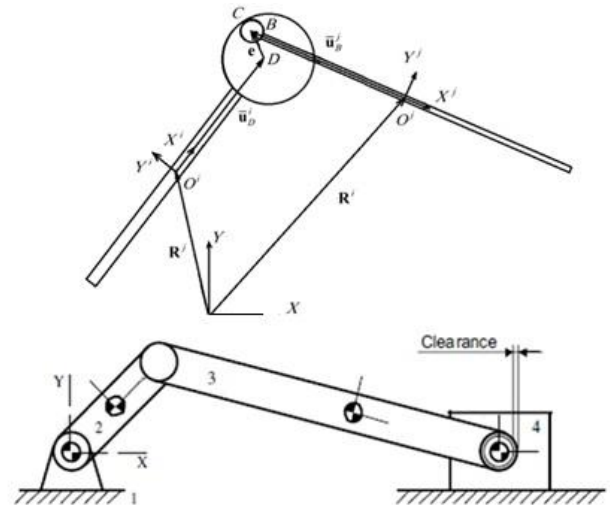


Fig. 2 Geometric description of a revolute clearance joint and a slider-crank with its reference coordinates (Flores and Ambrosio 2004)

the penetration velocity,  $\dot{\delta}^{(-)}$  is the initial penetration velocity,  $R_i$  and  $R_j$  are the radii of the journal and the bearing,  $\nu$  is the Poisson's ratio and  $E$  is the elastic modulus of the colliding bodies. To improve the model, the friction force is applied at the contact point. This force is calculated using a modification of Coulomb's friction law proposed in (Flores and Ambrosio 2004). This friction force is as follows

$$\mathbf{F}_T = -c_f c_d F_N \frac{\mathbf{v}_T}{|\mathbf{v}_T|} \quad (16)$$

where  $c_f$  is the coefficient of friction,  $\mathbf{v}_T$  is the relative tangential velocity and  $c_d$  is a dynamic correction coefficient which is expressed as

$$c_d = \begin{cases} 0 & \text{if } v_T \leq v_0 \\ \frac{v_T - v_0}{v_1 - v_0} & \text{if } v_1 \leq v_T \leq v_0 \\ 1 & \text{if } v_T \geq v_1 \end{cases} \quad (17)$$

where  $v_0$  and  $v_1$  are given tolerances for velocity (Flores 2004). In order to determine the direction of the contact force, the contact point and the amount of penetration has to be formulated. To do this, consider Fig. 2.

In this figure, two bodies which are joined together with a clearance revolute joint are shown. The eccentric vector is calculated as

$$\mathbf{e} = (\mathbf{R}^i + \mathbf{A}^i \bar{\mathbf{u}}_D^i) - (\mathbf{R}^j + \mathbf{A}^j \bar{\mathbf{u}}_B^j) \quad (18)$$

where  $\mathbf{R}^i$  and  $\mathbf{R}^j$  denote the vectors joining the global origin to the origins of body  $i$  and  $j$ , respectively.  $\mathbf{A}^i$  and  $\mathbf{A}^j$  are the transformation matrices from the body-fixed coordinates to the global reference frame.  $\bar{\mathbf{u}}_D^i$  and  $\bar{\mathbf{u}}_B^j$  are the local position vectors of the journal and bearing centers w.r.t the corresponding body-fixed coordinate systems. Now the position of the contact point is determined as follows

$$\mathbf{r}_c^k = \mathbf{R}^k + \mathbf{A}^k \bar{\mathbf{u}}^k + R_k \mathbf{n} \quad k = i, j \quad (19)$$

where  $\mathbf{r}_c^k$  is the position vector of the contact point w.r.t the journal or the bearing and  $\mathbf{n}$  is the unit vector in the direction of contact.

$$\mathbf{n} = \frac{\mathbf{e}}{e}, \quad e = |\mathbf{e}| \quad (20)$$

The penetration between journal and bearing is calculated as

$$\delta = e - (R_j - R_i) \quad (21)$$

The penetration velocity is required to determine the contact force and it is achieved as

$$\dot{\mathbf{r}}_c^k = \dot{\mathbf{R}}^k + \dot{\theta}_k \mathbf{A}_\rho^k \bar{\mathbf{u}}^k + R_k \dot{\mathbf{n}} \quad k = i, j \quad (22)$$

where  $\mathbf{A}_\rho^k$  is the derivative of the transformation matrix w.r.t. the body-fixed frame orientation. Then the normal and tangential penetration velocities are computed as

$$\begin{aligned} \mathbf{v}_n &= (\dot{\mathbf{r}}_c^i - \dot{\mathbf{r}}_c^j) \cdot \mathbf{n} \\ \mathbf{v}_t &= (\dot{\mathbf{r}}_c^i - \dot{\mathbf{r}}_c^j) \cdot \mathbf{t} \end{aligned} \quad (23)$$

where  $\mathbf{t}$  is the tangential unit vector. Having obtained the contact force, it must be added to the generalized external vector in Eqs. (5)-(11). To do this, the contact force is transferred to the origin of the colliding bodies reference frame and it requires considering the moment of the contact force.

### 3.1 Contact detection

Determining the instant of contact in multibody systems with clearance is necessary. In addition, calculation of the contact force requires knowing the pre-impact conditions. In this paper, the second strategy suggested by Flores and Ambrosio (2010) is used to estimate the instant of contact. In this strategy, when the penetration sign changes from negative to positive, i.e., contact is happening, the step time for integration of the equations of motion is reduced, and it continues until the penetration becomes less than a predetermined value. This time is taken as the impact time and the penetration velocity is used to calculate the contact force.

## 4. Energy characterization

Kinetic and potential energies of a multibody system are added to constitute the total energy of the system. The kinetic energy is calculated as

$$K.E = \frac{1}{2} \dot{\mathbf{q}}^T \mathbf{M} \dot{\mathbf{q}} \quad (24)$$

where  $\mathbf{M}$  is the mass matrix of the system and  $\dot{\mathbf{q}}$  is the vector of generalized velocities of the system. The potential energy of the system is calculated as

Table 1 Properties of the slider-crank mechanism

	crank	coupler	slider
Length (cm)	5	12	-
Mass (kg)	0.3	0.21	0.14
Mass moment of inertia (kg.m <sup>2</sup> )	0.0001	0.00025	0.0001

$$P.E = \sum_{i=1}^{n_b} m_i g h_i + \frac{1}{2} \mathbf{q}^T \mathbf{K} \mathbf{q} \quad (25)$$

where  $n_b$  is the total number of bodies. The first term is the gravitational potential energy and the second one indicates the strain energy related to the flexible bodies. Apparently, when the multibody system is assumed to be rigid, the second term vanishes.

## 5. Application to a slider-crank mechanism

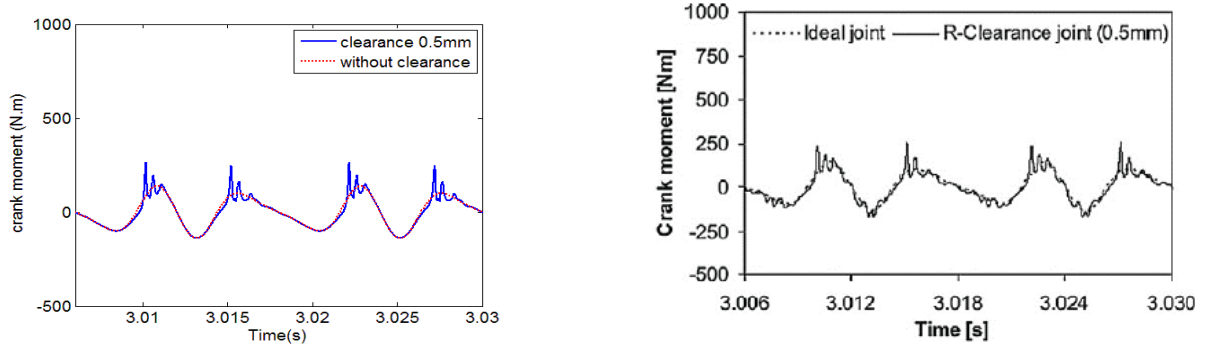
To investigate the effect of clearance on the energy of a multibody system, a slider-crank is used as an example (Fig. 2). Table 1 shows the properties of this mechanism.

The modulus of elasticity of the slider and coupler is  $E=207$  Gpa, the poisson's ratio is  $\nu=0.3$ , and the coefficient of restitution is  $e_r=0.9$ . The revolute joint between the slider and the coupler is assumed to be non-ideal. The radius of the bearing is 10 mm and the clearance varies to see its effect on the energy of the system. The crank rotates with an initial angular velocity and the initial crank angle is supposed to be  $0^\circ$ . The reason for considering the initial angular velocity without applying any moment to the crank is that the energy is the subject of interest and it is assumed that no external energy is given to the system. When clearance exists, the initial conditions are assumed to be the same as the ones when the joints are ideal and the centers of the journal and the bearing are coincident initially. The Runge-Kutta-Fehlberg method was used to integrate the equations of motion (Schiling and Harris 1999). In order to prevent constraint violation, the coordinate partitioning technique proposed by Wehage, was used in which the independent accelerations were separated from the dependent ones and integrated forward to obtain the independent coordinates and velocities (Shabana 2001).

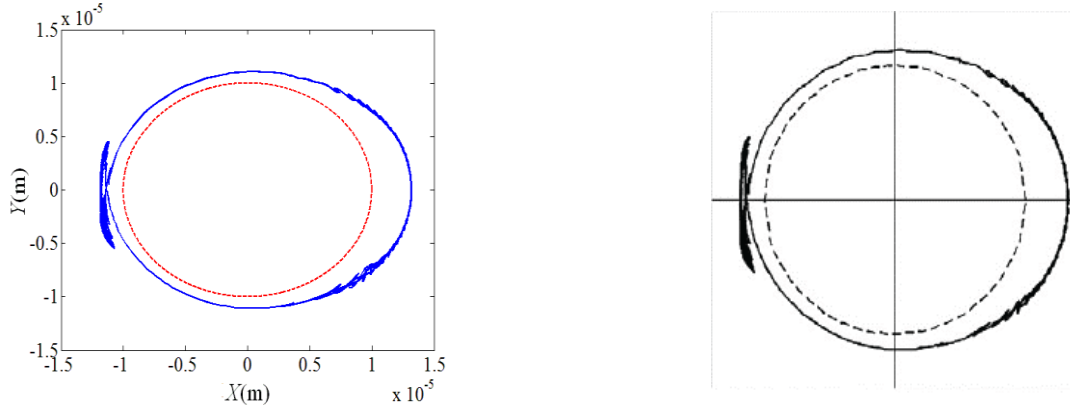
### 5.1 Results and discussion

#### 5.1.1 Dynamic response Validation of the model

At first, the dynamic response of the rigid system is compared with the literature. For this purpose, a crank slider having a clearance in the joint between the slider and the coupler with the properties of Table 1 taken from Flores and Ambrosio (2004) is considered. The journal trajectory inside the bearing is plotted in Fig. 3(a) for clearance 0.01 mm and without friction. In addition, the crank moment applied for obtaining the constant crank angular velocity (5000 rpm) is plotted in Fig. 3(b) for clearance 0.5 mm and coefficient of friction 0.1. As it can be seen, an acceptable agreement exists between the results of the rigid system formulation presented here and those of the literature



(a) left plot: our simulation, right plot: results of simulation from Flores and Ambrosio (2004)



(b) left plot: our simulation, right plot: results of simulation from Flores and Ambrosio (2004)

Fig. 3 Comparison of the results with Flores and Ambrosio (2004): (a) crank moment for clearance 0.5 mm and coefficient of friction 0.1, (b) journal center trajectory inside the bearing for clearance 0.01 mm and without friction

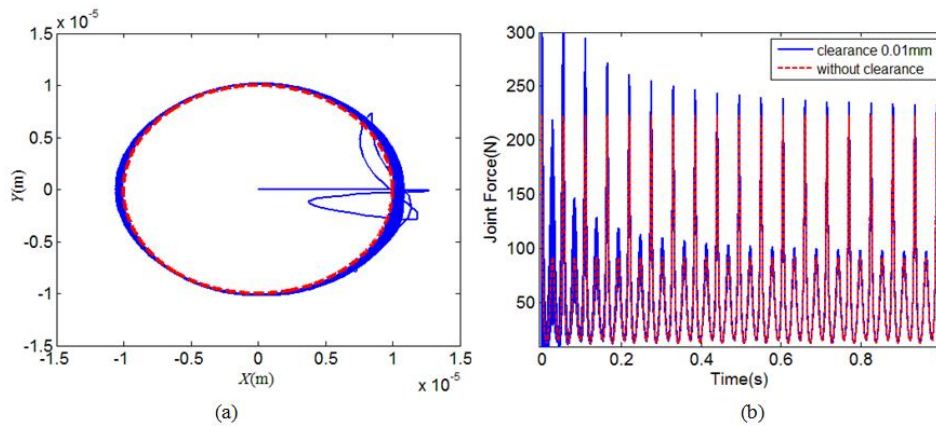


Fig. 4 (a) Journal center trajectory with respect to the bearing with and without clearance, (b) The joint force in two cases, with and without clearance

(Flores and Ambrosio 2004).

Dynamic response with initial angular velocity

As mentioned, the crank rotates with an initial angular velocity to facilitate analyzing the energy of the system. In this part, the dynamic response is plotted for the initial angular velocity 150 rad/s and coefficient of restitution 0.8. The clearance is set to be 0.01 mm and the friction is neglected. The journal trajectory and the joint reaction force in the joint between slider and the coupler in two cases, with and without clearance, are plotted in Figs. 4(a)-(b), respectively. After four impacts, the journal and the bearing

enter and stay in the continuous contact mode. In the transient response, the contact force is relatively high, but then it reduces. As it can be seen, the contact force model is able to model the joint reaction force in a good manner.

In addition, it is expected that the joint force reduces gradually in comparison with the case no clearance exists. The reason refers to this fact that in the clearance model, the hysteresis damping is considered which reduces the energy of the system. This energy dissipation is not considered when the system is modeled as if there is no clearance. The peaks of the joint force in the case of clearance come down gradually in the first second which could be the result of

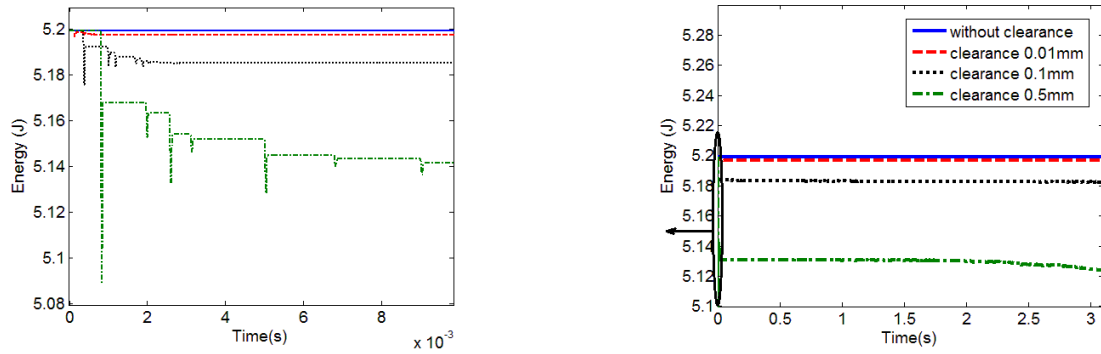


Fig. 5 The energy of the system for different clearance sizes neglecting the friction

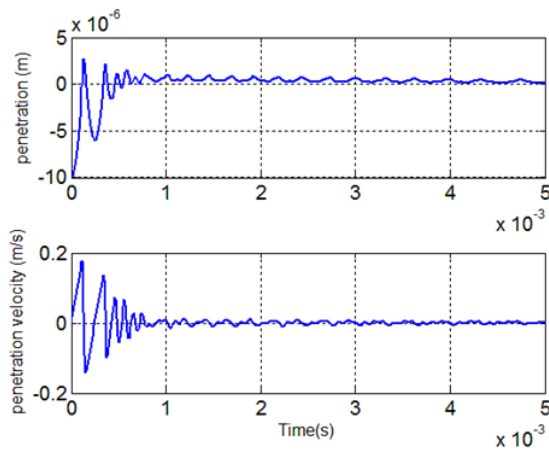


Fig. 6 Penetration and penetration velocity at the beginning of the motion

clearance damping.

The effect of the clearance size

In this section, a comparison between the total energy (sum of the kinetic and potential energies) of the slider-crank without clearance and the one with a clearance between the slider and the coupler is made. For this purpose, different clearance sizes are used for simulation. The crank initial angular velocity is set to be 150 rad/s counterclockwise, the coefficient of restitution is 0.8 and the friction is neglected. The simulations were done for three clearance sizes, 0.01 mm, 0.1 mm and 0.5 mm. The results are shown in Fig. 5.

When there is no clearance, the total energy is constant as expected. This is due to this fact that there is no source of energy dissipation. As it can be seen, the reduction rate of the system energy with clearance size of 0.5 mm is approximately more than other clearance sizes. When the

slider-crank starts to move, a sudden change in the energy happens in comparison with the case of no clearance.

This sudden change occurs because at the beginning of the motion, some impacts happen until the journal goes to the continuous contact mode. These impacts cause a relatively large penetration and penetration velocity. As a result, a sudden reduction in the energy could happen due to the hysteresis damping considered in the contact force model. These relatively large penetration and penetration velocity are shown in Fig. 6.

It is noteworthy that the horizontal parts of the zoomed area of the energy diagram correspond to the free flight motion in which there is no contact between the journal and the bearing and hence no energy loss will exist. The oscillation of the amount of energy is due to the first term of the contact force which plays the role of a nonlinear spring. When penetration takes place, this spring absorbs the energy and then gives it back when the penetration reduces. However, the level of the total energy does not return to its initial level before penetration because of the energy dissipation during contact. The number of collisions between the journal and the bearing are 4, 19 and 33 for clearance sizes 0.01 mm, 0.1 mm and 0.5 mm, respectively. This could be a reason for more sudden reduction in the energy of the system at the beginning of the motion for clearance size 0.5 mm.

The effect of the crank initial angular velocity

In this section, the effect of initial angular velocity of the crank on the energy of the slider-crank mechanism is investigated. The clearance is 0.01 mm and the friction is neglected. As shown in Fig. 7, increasing the initial angular velocity of the crank yields a sudden change of the energy at the beginning. Table 2 shows the amount of energy reduction in the interval of 0.05s at the beginning of the motion for different initial crank angular velocities.

Table 2 Energy loss in the interval of 0.05s at the beginning of the motion for different initial crank angular velocities

Initial crank angular velocity (rad/s)	Energy of the mechanism at the beginning of the motion (J)	Energy of the mechanism at the end of the period (J)	Energy loss (J)	Energy loss ratio	Number of collisions in this period
50	0.5777	0.5775	0.0002	0.034620%	29
100	2.3108	2.3100	0.0008	0.034620%	22
150	5.1992	5.1973	0.0019	0.036544%	4
200	9.2431	9.2393	0.0038	0.041112%	3

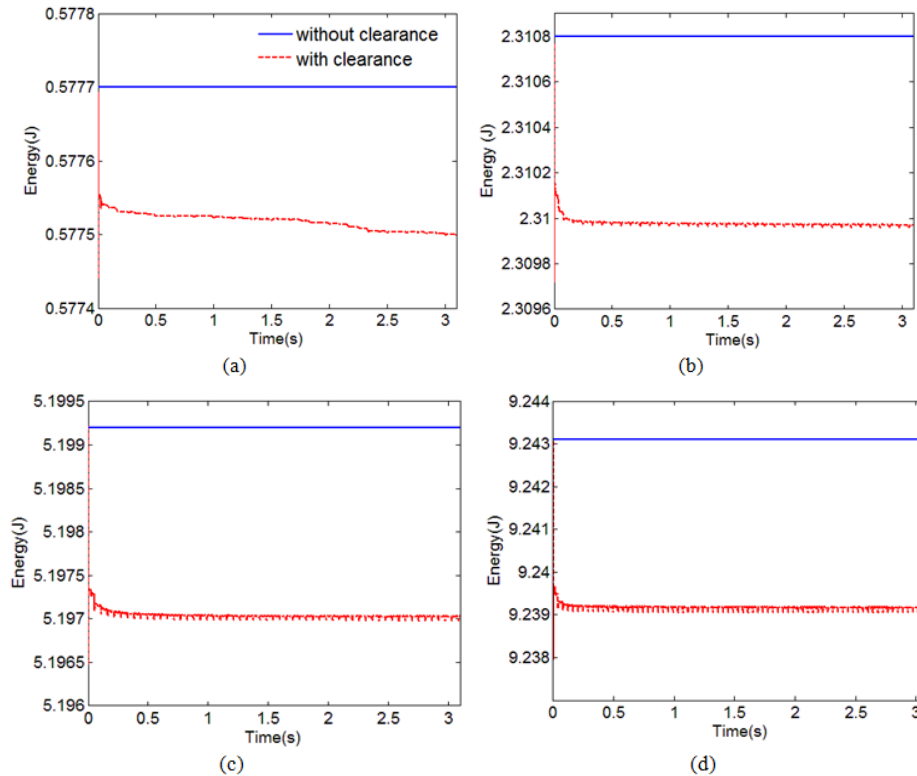


Fig. 7 Energy of the system for different crank initial angular velocities: (a) 50 rad/s, (b) 100 rad/s, (c) 150 rad/s and (d) 200 rad/s

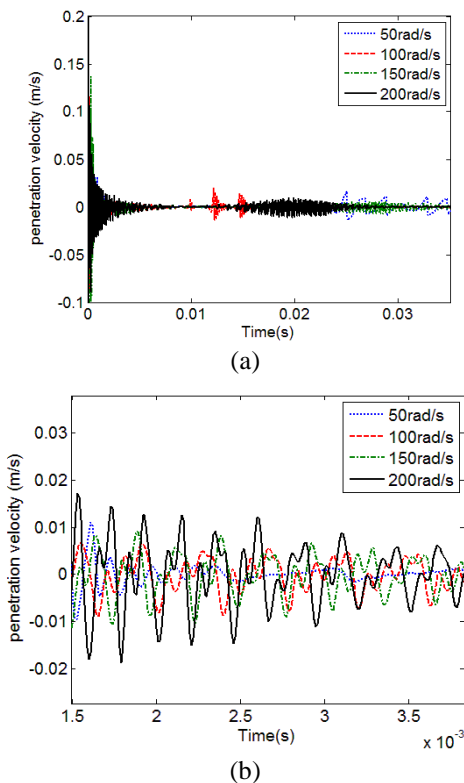


Fig. 8 Penetration velocity for different initial crank angular velocities: (a) overall view, (b) zoomed view

Although the number of collisions decreases as the initial crank angular velocity increases, the energy loss increases.

The amount of penetration velocity could be the reason as the equation of contact force (Eq. (15)) indicates.

The penetration velocity for different initial crank angular velocities is shown in Fig. 8. It can be concluded that the value of the penetration velocity changes more frequently for the initial angular velocity 200 rad/s and it has the maximum value in some parts of the diagram.

The effect of the coefficient of friction

In this section, the effect of changing the coefficient of friction between the journal and the bearing, on the energy of the slider-crank is investigated. The clearance is chosen to be 2 mm and the initial crank angular velocity is set to be 300 rad/s. As shown in Fig. 9(a), increasing the coefficient of friction up to 0.1 increases the energy loss, too. This result could be expected due to the role of the friction in energy loss. However, further increase of the coefficient of friction decreases the energy loss which is surprising. The reason could refer to this issue that when the coefficient of friction increases, the tangential velocity of the journal relative to the bearing decreases, too. Therefore, the dynamic correction coefficient ( $c_d$ ) which varies linearly between two tolerances for velocities (in this example  $v_0=0.001$  m/s and  $v_1=0.01$  m/s), decreases, too. The tangential velocity of the journal relative to the bearing for four coefficients of friction is plotted in Figs. 9(b)-(c) for a part of the simulation.

The effect of the initial configuration

In this section, two cases are compared with each other: In the first case, the journal and the bearing are initially

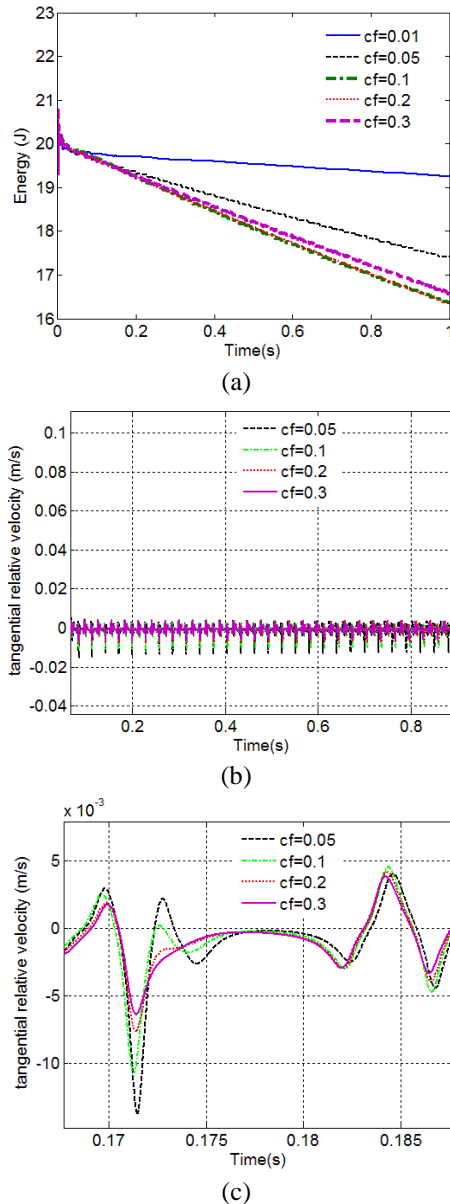


Fig. 9 (a) Energy of the slider-crank mechanism with clearance joint for different coefficients of friction, (b)-(c) Journal tangential velocity relative to the bearing

concentric and in the second one the journal is very close to the bearing wall (near contact,  $e = -1 \times 10^{-8}$  m (clearance)) at the start of the motion (Fig. 10). The reason that the journal and the bearing are chosen to be initially very close rather than to be in contact, lies in the contact force model formulation (Eq. (15)) which depends on the impact velocity that has to be determined at the moment of the contact. It is important to note that the crank starts to rotate counterclockwise. The clearance size, crank initial angular velocity and coefficient of the friction are set to be 2mm, 300rad/s and 0.01, respectively.

The result is shown in Fig. 11. As expected, at the beginning of the motion, the case in which the journal and the bearing are farther away from each other (concentric case), the reduction in the amount of energy of the system is more.

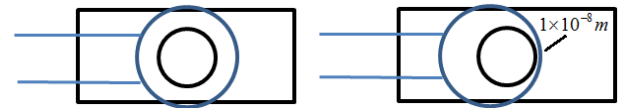


Fig. 10 Two initial configurations of the journal and the bearing

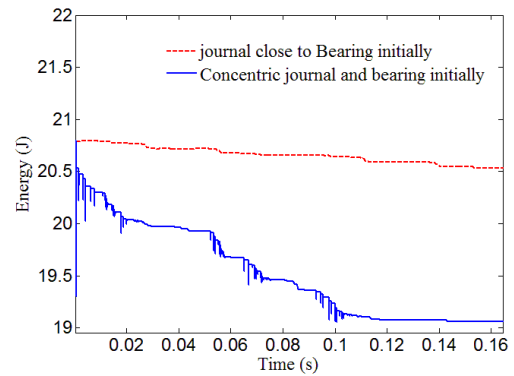


Fig. 11 Energy of the mechanism for two different initial configurations

#### The effect of the coupler flexibility

In this section, the coupler of the mechanism is considered as a flexible body. One element was used to model the flexibility of the coupler. The initial crank angular velocity is 150 rad/s, the clearance size is 0.01 mm, the friction is neglected, the coupler diameter is 1cm and the damping ratios are set to be 0.04. The integration time step for the continuous contact mode is considered to be 0.00001s. A comparison between two cases, the rigid and the flexible couplers, is made and the result is shown in Fig. 12(b). As it can be seen, clearance has a considerable effect on the energy loss in the case of flexible coupler, too. Comparing these two cases shows that the energy loss for the flexible coupler case is more than that of the rigid one. This could be the result of flexibility (internal damping) of the coupler. The rate of the energy reduction for the mechanism with flexible coupler in two cases, with and without clearance, is nearly the same after the impacts finish. At this time, the journal and the bearing enter the continuous contact mode. At the beginning of the motion (see Fig. 12(c)), there are energy reduction jumps which are higher for the rigid case.

The reason is clarified when paying attention to the amount of penetration for the two cases shown in Fig. 12(d). In the flexible coupler case with clearance size of 0.01 mm, the amount of penetration is lower than that of the rigid one at the start of the motion. This can be due to the effect of coupler flexibility which makes it as a suspension for the mechanism (Khemili and Romdhane 2008). In addition, taking a look at the journal trajectory for two cases (Fig. 12(d)), reveals that the amount of penetration is lower when the coupler is considered as a flexible beam. This could be the reason for higher reduction of the energy at the start of the motion for the rigid case.

#### Energy loss: hysteresis damping, friction and Rayleigh damping

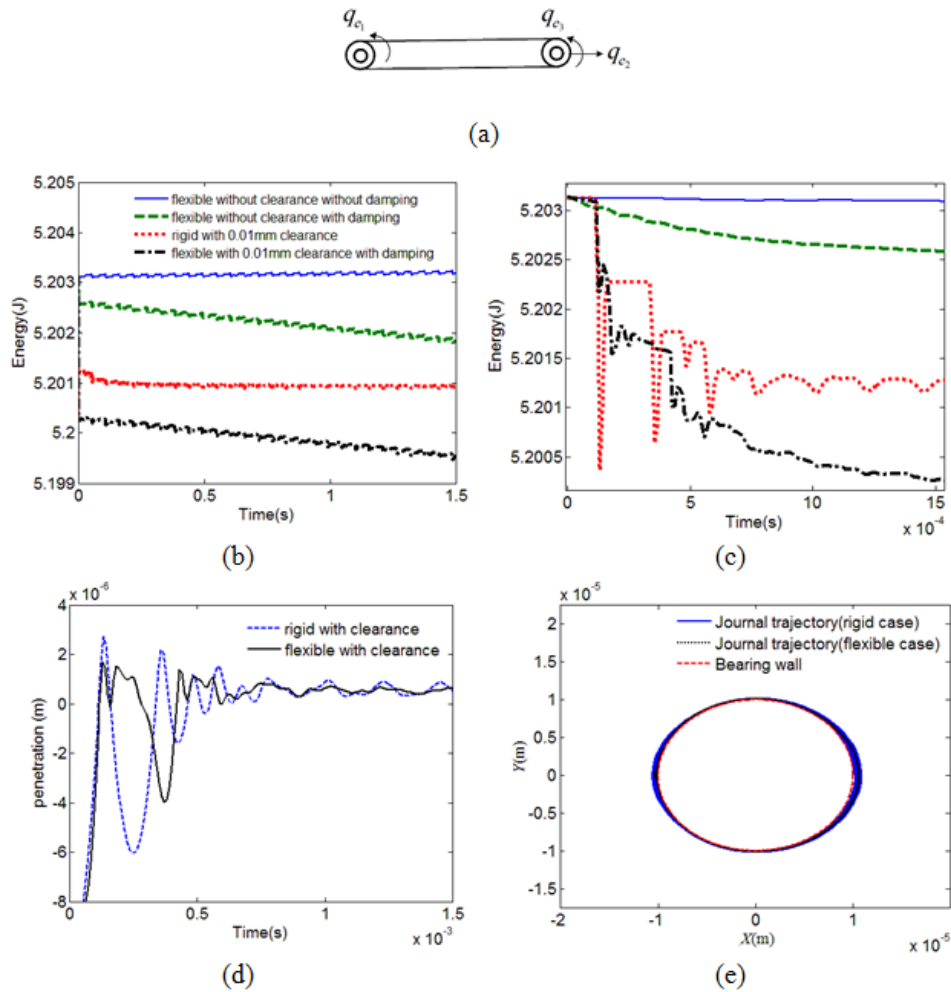


Fig. 12 (a) Elastic coordinates of the coupler used in the floating frame of reference formulation, (b) The energy of the slider-crank mechanism for two cases, rigid and flexible coupler, (c) The energy of the slider-crank mechanism for two cases, rigid and flexible coupler at the beginning of the motion, (d) The amount of penetration for two cases, rigid and flexible coupler, and (e) The journal trajectory inside the bearing for two cases, rigid and flexible couplers

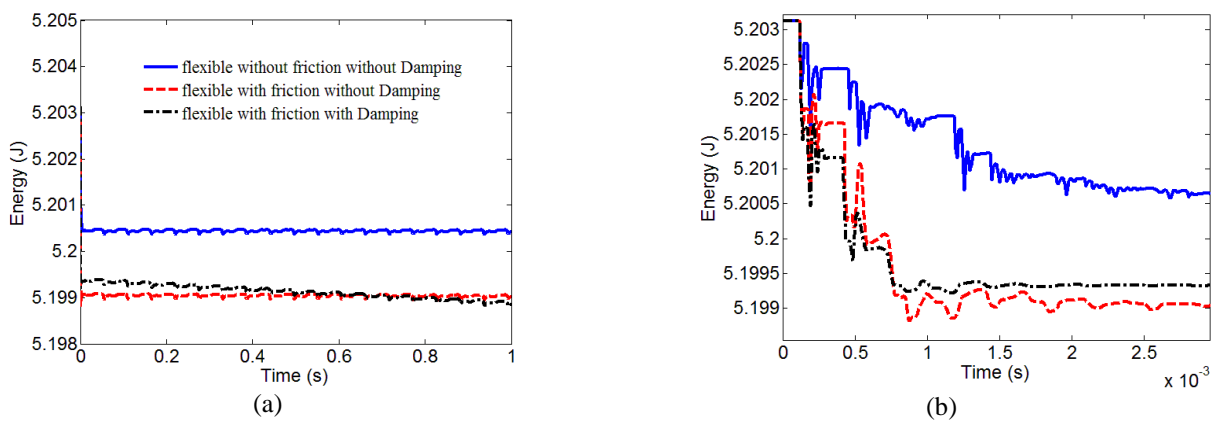


Fig. 13 (a) Energy variation of the mechanism for three cases, without friction, with friction, and with both friction and Rayleigh damping, (b) zoomed part of it (the start of the motion)

Finally, three cases are compared with each other for the flexible slider-crank mechanism with a single clearance joint to observe the effect of any causes of the energy dissipation: hysteresis damping, friction and Rayleigh damping. In the first case, no friction and no Rayleigh

damping is considered. In the second one, friction is included and for the third one, Rayleigh damping is also taken into account. The clearance size, the initial crank angular velocity, the coefficient of restitution and the coefficient of friction are set to be 0.01 mm, 150 rad/s, 0.9

Table 3 Energy loss ratio for three cases

Case No.	Energy of the mechanism (J) at $t=0.05s$	Energy of the mechanism (J) at $t=1s$	Energy loss(J)	Energy loss ratio
1	5.200474351	5.20042468	0.000049671	0.000955 %
2	5.1990824	5.19901588	0.00006652	0.00128 %
3	5.19939	5.198854	0.000536	0.0103 %

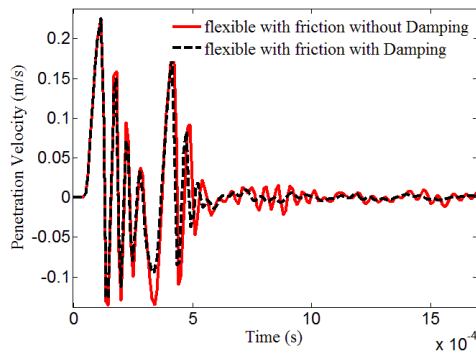


Fig. 14 The penetration velocity for the second case (with friction) and the third case (with both friction and Rayleigh damping)

and 0.1, respectively. The energy variation for these cases is shown in Fig. 13. As can be seen, in the beginning of motion, the third case dissipates more energy than the others and so, does the second one more than the first one. However, the third case reaches an upper level than the second case after the initial sudden changes finish. The reason may be found by inspecting the penetration velocity of the two cases in Fig. 14. From Fig. 14, one can find that the penetration velocity for the third case is totally lower than the second one. This was expected since the coupler flexibility plays the role of suspension for the mechanism (Khemili and Romdhane 2008) and it can reduce the rate of penetration of the journal into the bearing.

Table 3 shows the energy loss ratio for these three cases between  $t=0.05s$  and  $t=1s$ . As can be seen, when the Rayleigh damping of the coupler is included, the most energy loss ratio is observed in comparison with the energy loss ratio due to the hysteresis damping and friction caused by contact.

## 6. Conclusions

The effect of the joint clearance on the amount of energy loss of a slider-crank mechanism was investigated. The contact force model was based on the Lankarani and Nikravesh model and the friction force was calculated using the modified Coulomb's friction law. The hysteresis damping included in the contact force model, dissipates energy in clearance joints. The other reason for the energy loss is the friction between the journal and the bearing.

- It was shown that the energy reduction of the system at the start of the motion is more for higher initial crank angular velocities and clearance sizes.
- In addition, it was concluded that the more the coefficient of friction was, the more energy loss would be up to a coefficient of friction 0.1.

- Then the effect of initial configuration on the energy of the mechanism was studied. It was found that at the beginning of the motion, the case in which the journal and the bearing are initially farther away from each other (concentric case) reduction in energy of the system is more.

- The effect of the coupler flexibility on the energy of the system was investigated. The energy loss for the flexible coupler case was more than that of the rigid one. In addition the lower energy reduction jump happened for the flexible case at the start of the motion. This happened due to the role of the coupler flexibility as a suspension which made the amount of penetration lower at the start of the motion when the impact occurs.

- Finally, it was illustrated that when the Rayleigh damping of the coupler is included, the most energy loss ratio is observed in comparison with the energy loss ratio due to the hysteresis damping and friction caused by contact.

## References

- Bathe, K.J. (1996), *Finite Element Procedures*, Prentice-Hall Inc, New Jersey, USA.
- Chunmei, J., Yang, Q., Ling, F. and Ling, Z. (2002), "The non-linear dynamic behavior of an elastic linkage mechanism with clearances", *J. Sound Vib.*, **249**(2), 213-226.
- Dubowsky, S. and Freudenstein, F. (1971), "Dynamic analysis of mechanical systems with clearances, Part I: Formation of dynamic model", *J. Eng. Indust.*, 305-309.
- Ebrahimi, S., Salahshoor, E. and Moradi, S. (2017a) "Vibration performance evaluation of planar flexible multibody systems with joint clearance", *J. Braz. Soc. Mech. Sci. Eng.*, 1-15.
- Ebrahimi, S., Salahshoor, E. and Maasoomi, M. (2017b), "Application of the method of multiple scales for nonlinear vibration analysis of mechanical systems with dry and lubricated clearance joints", *J. Theor. Appl. Vib. Acoust.*, **3**(1), 42-61.
- Ebrahimi, S. (2007), "A contribution to computational contact procedures in flexible multibody systems", Ph.D. Dissertation, Institute of Engineering and Computational Mechanics, University of Stuttgart, Germany.
- Ebrahimi, S. and Eberhard, P. (2008), "Aspects of linear complementarity problems on position and velocity level in normal impact formulation of planar deformable bodies", *MMMS Int. J. Multidisc. Model. Mater. Struct.*, **4**, 331-344.
- Erkaya, S. and Uzmay, I. (2009), "Optimization of transmission angle for slider-crank mechanism with joint clearances", *Struct. Multidisc. Optim.*, **37**, 493-508.
- Erkaya, S. (2012), "Prediction of vibration characteristics of a planar mechanism having imperfect joints using neural network", *J. Mech. Sci. Technol.*, **26**, 1419-1430.
- Feng, B.Z., Yang, Z. and Gui, W.X. (2013), "Wear analysis of revolute joints with clearance in multibody systems", *Phys. Mech. Astron.*, **56**, 1581-1590.

- Flores, P. and Ambrosio, J. (2004), "Revolute joints with clearance in multibody systems", *Comput. Struct.*, **82**, 1359-1369.
- Flores, P., Ambrosio, J. and Claro, J.P. (2004), "Dynamic analysis for planar multibody mechanical systems with lubricated joints", *Multib. Syst. Dyn.*, **12**, 47-74.
- Flores, P. (2004), "Dynamic analysis of mechanical systems with imperfect kinematic joints", Ph.D. Dissertation, University of Minho, Braga, Portugal.
- Flores, P. and Ambrosio, J. (2010), "On the contact detection for contact-impact analysis in multibody systems", *Multib. Syst. Dyn.*, **24**(1), 103-122.
- Gandhi, V.C. Sathish, Kumaravelan, R., Ramesh, S. and Sriram, K. (2015), "Analysis of material dependency in an elastic - plastic contact models using contact mechanics approach", *Struct. Eng. Mech.*, **53**(5), 1051-1066.
- Garrido, J.A., Foces, A. and Paris, F. (1994), "An incremental procedure for three-dimensional contact problems with friction", *Comput. Struct.*, **50**(2), 201-215.
- Jablokow, A.G., Nagarajan, S. and Turcic, D.A. (1993), "A modal analysis solution technique to the equations of motion for elastic mechanism systems including the rigid-body and elastic motion coupling terms", *Tran. ASME, J. Mech. Des.*, **115**, 314-323.
- Khemili, I. and Romdhane, L. (2008), "Dynamic analysis of a flexible slider-crank mechanism with clearance", *Euro. J. Mech. A Solid.*, **27**, 882-898.
- Lankarani, H.M. and Nikravesh, P. (1994), "Continuous contact force models for impact analysis in multibody systems", *Nonlin. Dyn.*, **5**, 193-207.
- Li, C., He, Y. and Ning, X. (2015), "Helical gear multi-contact tooth mesh load analysis with flexible bearings and shafts", *Struct. Eng. Mech.*, **55**(4), 839-856.
- Liu, Z. and Yang, Y. (1998), "Contact surface element method for two-dimensional elastic contact problems", *Struct. Eng. Mech.*, **6**(4), 363-375.
- Mukras, S., Kim, N.H., Mauntler, N.A., Schmitz, T.L. and Sawyer, W.G. (2010), "Analysis of planar multibody systems with revolute joint wear", *Wear*, **268**, 643-652.
- Oner, E., Yaylaci, M. and Birinci, A. (2015), "Analytical solution of a contact problem and comparison with the results from FEM", *Struct. Eng. Mech.*, **54**(4), 607-622.
- Pei, L., Wei, C. and Bin, Z. A. (2013), "An improved practical model for wear prediction of revolute clearance joints in crank slider mechanisms", *Sci. China Press Springer-Verlag Berlin Heidelberg* **56**(2), 2953-2963.
- Rahmanian, S. and Ghazavi, M.R. (2015), "Bifurcation in planar slider-crank mechanism with revolute clearance joint", *Mech. Mach. Theor.*, **91**, 86-101.
- Ravn, P. (1998), "A continuous analysis method for planar multibody systems with joint clearance", *Multib. Syst. Dyn.*, **2**, 1-24.
- Rhee, J.K. and Akay, A. (1996), "Dynamic response of a revolute joint with clearance", *J. Mech. Mach. Theor.*, **31**, 121-134.
- Salahshoor, E., Ebrahimi, S. and Maasoomi, M. (2016), "Nonlinear vibration analysis of mechanical systems with multiple joint clearances using the method of multiple scales", *Mech. Mach. Theor.*, **105**, 495-509.
- Sardashti, A., Daniali, H.M. and Varedi, S.M. (2013), "Optimal free-defect synthesis of four-bar linkage with joint clearance using PSO algorithm", *Meccanica*, **48**, 1681-1693.
- Schilling, R.J. and Harris, S.L. (1999), *Applied Numerical Methods for Engineering*, CL Engineering, Brooks/Cole.
- Schwab, A.L., Meijaard, J.P. and Meijers, P. (2002), "A comparison of revolute joint clearance models in the dynamic analysis of rigid and elastic mechanical systems", *Mech. Mach. Theor.*, **37**, 895-913.
- Shabana, A.A. (2001), *Computational Dynamics*, John Wiley & Sons, Inc, New York, USA.
- Shabana, A.A. (2005), *Dynamics of Multibody Systems*, Cambridge University Press, New York, USA
- Tian, Q., Zhang, Y., Chen, L. and Flores, P. (2009) "Dynamics of spatial flexible multibody systems with clearance and lubricated spherical joints", *Comput. Struct.*, **87**(13-14), 913-929.
- Tian, Q., Zhang, Y., Chen, L. and Yang, J.J. (2010) "Simulation of planar flexible multibody systems with clearance and lubricated revolute joints", *Nonlin. Dyn.*, **60**(4), 489-511.
- Tian, Q., Liu, C., Machado, M. and Flores, P. (2011) "A new model for dry and lubricated cylindrical joints with clearance in spatial flexible multibody systems", *Nonlin. Dyn.*, **64**(1-2), 25-47.
- Tian, Q., Sun, Y., Liu, C., Hu, H. and Flores, P. (2013) "Elastohydrodynamic lubricated cylindrical joints for rigid-flexible multibody dynamics", *Comput. Struct.*, **114-115**, 106-120.
- Tian, Q., Xiao, Q., Sun, Y., Hu, H., Liu, H. and Flores, P. (2015) "Coupling dynamics of a geared multibody system supported by ElastoHydroDynamic lubricated cylindrical joints", *Multib. Syst. Dyn.*, **33**(3), 259-284.
- Vaidya, A.M. and Padole, P.M. (2010), "A performance evaluation of four bar mechanism considering flexibility of links and joints stiffness", *Open Mech. Eng. J.*, **4**, 16-28.
- Varedi, S.M., Daniali, H.M., Dardel, M. and Fathi, A. (2015), "Optimal dynamic design of a planar slider-crank mechanism with a joint clearance", *Mech. Mach. Theor.*, **86**, 191-200.
- Yang, G., Yang, J., Qiang, C., Ge, J. and Chen, Q. (2012), "Natural frequencies of a cantilever beam and block system with clearance while block staying on given position", *J. Vib. Control*, **19**, 262-275.
- Zhang, X., Zhang, X. and Chen, Z. (2014), "Dynamic analysis of a 3-RRR parallel mechanism with multiple clearance joints", *Mech. Mach. Theor.*, **78**, 105-115.
- Zhang, Z., Xu, L., Tay, Y.Y., Flores, P. and Lankarani, H. (2015), "Multi-objective optimization of mechanisms with clearances in revolute joints", *Mech. Mach. Sci.*, **24**, 423-433.
- Zhao, B., Zhang, Z.N. and Dai, X.D. (2013), "Prediction of wear at revolute clearance joints in flexible mechanical systems", *Procedia Eng.*, **68**, 661-667.
- Zhao, Y., Zhang, B., An, G., Liu, Z. and Cai, L. (2016), "A hybrid method for dynamic stiffness identification of bearing joint of high speed spindles", *Struct. Eng. Mech.*, **57**(1), 141-159.

CC